Reversal of OFI and CHF in Research Reactors Operating at 1 to 50 bar

M. Kalimullah, A. P. Olson, B. Dionne, E. E. Feldman, and J. E. Matos
GTRI Program, Nuclear Engineering Division, Argonne National
Laboratory, 9700 S. Cass Avenue, Argonne IL 60439 – USA

ABSTRACT

The condition at which the critical heat flux (CHF) and the heat flux at the onset of Ledinegg flow instability (OFI) are equal, is calculated for a coolant channel with uniform heat flux as a function of five independent parameters: the channel exit pressure (P), heated length (L_h), heated diameter (D_h), inlet temperature (T_{in}), and mass flux (G). A diagram is made by plotting the mass flux and heat flux at the OFI-CHF intersection (i.e., reversal from CHF > OFI to CHF < OFI as G increases) as a function of P (1 to 50 bar), for 36 combinations of the remaining 3 parameters (L_h , D_h , T_{in}). The application of the diagram *to scope* whether a research reactor is OFI-limited (below the curve) or CHF-limited based on the five parameters of its most-limiting coolant channel is described. Justification for application of the diagram to research reactors with axially non-uniform heat flux is provided.

In order to make the OFI-CHF intersection diagram, two world-class CHF prediction methods (the Hall-Mudawar inlet-conditions correlation and the extended Groeneveld 2006 Table) are compared for 216 combinations of the five independent parameters. Also, two widely used OFI correlations (the Saha-Zuber and the Whittle-Forgan with η = 32.5) are compared for the same combinations of the five parameters. The extended Groeneveld Table and the Whittle-Forgan OFI correlation are selected and used in making the diagram. Using the five design parameters, the operating state of any research reactor can be located on the reversal diagram that will readily show whether CHF or OFI is most-limiting. The scoping results of the OFI-CHF diagram for five research reactors (ATR, HIFR, MITR, MURR, and the ANS Design) are found to agree with the results reported by their owners. Due to its limitations (uncertainties not included), the diagram cannot replace the detailed thermal-hydraulic analysis required for a reactor safety analysis.

1. Introduction

Safe operation of a research reactor requires establishing an operational envelope that maintains sufficient margins to unsafe conditions, e.g., fuel plate overheating. Two key phenomena that can cause unsafe conditions in research reactors are Critical Heat Flux (CHF), and Onset of Flow

Instability (OFI). It is well known that OFI is most limiting for many research reactors. However, as the operating regime of channel exit pressure and mass flux changes from reactor to reactor, there is a cross-over beyond which CHF is most limiting. An understanding and quantification of this OFI-CHF cross-over may provide information useful in the conversion of research reactors, including the US High Performance Research Reactors (US-HPRRs). The purpose of this work (summarized from Ref. 1) is to provide an understanding and quantification of OFI-CHF cross-over in terms of the thermal-hydraulic parameters of coolant channel.

The heat fluxes at the onset of nucleate boiling (ONB)[2,3], the onset of flow instability (OFI)[4,5,6], and the critical heat flux (CHF)[7,8,9] were calculated using the state-of-the-art methods, for heated lengths of 0.28, 0.61, and 1.18 m (about 11, 24, 46.5 inches), over the coolant mass flux range of 1000 to 30000 kg/m^2-s (i.e., the coolant velocity range of roughly 1 to 30 m/s), assuming uniform heat flux. These heat fluxes were calculated for 216 cases ranging over the existing research reactors' exit pressures (1 to 50 bar), fueled lengths, channel thicknesses, coolant velocities, and inlet temperatures. By investigating the relative magnitudes of the calculated heat fluxes, the OFI heat flux and CHF are found to intersect at a certain mass flux which depends on four parameters (i.e., P, L_h, D_h, T_{in}). This intersection, called OFI-CHF reversal point, is studied in this work.

For each heated length, a pair of OFI-CHF reversal diagrams (Fig. 4) is made by plotting the mass flux at the OFI-CHF intersection (G_{rev}) as function of exit pressure in one diagram, and by plotting the heat flux at the OFI-CHF intersection (q_{rev}) in the accompanying diagram. A given research reactor is represented by a point on these diagrams. The location of the point on the reversal mass flux diagram determines whether the maximum allowed power of the reactor is OFI-limited or CHF-limited. For demonstration, some research reactors are represented on the G_{rev} diagram. The value of the heat flux at the OFI-CHF reversal can also be read from the accompanying q_{rev} diagram.

2. Best Estimates of CHF and Heat Flux at OFI

The following five safety margins were calculated in a coolant channel using Eqs. (1) to (5), assuming axially uniform heat flux. With uniform heat flux, the ONB, OFI and CHF all occur at the channel exit. Each of these safety margins depends on five independent parameters of the channel: (1) coolant exit pressure (P), (2) heated diameter (D_h), (3) heated length (L_h), (4) inlet temperature (T_i), (5) mass flux (G).

(1) Heat flux at ONB using the Bergles and Rohsenow correlation [2, 3]
(2) Heat flux at OFI using $\eta = 32.5$ in the Whittle-Forgan correlation [4]
(3) Heat flux at OFI using the Saha-Zuber correlation [5, 6]
(4) Critical heat flux using the *extended* Groeneveld 2006 Table [7, 8]
(5) Critical heat flux using the Hall-Mudawar inlet conditions correlation (ICC) [9]

$$q_{ONB} \ (kW/m^2) = 1082.9 \times 10^{-3} \ P^{\,1.156} \ (1.8 \ \Delta T_{sat})^x \quad \text{where} \quad x = 2.16/P^{0.0234} \tag{1}$$

$$q_{OFI-WF} = \frac{D_h \ G \ (h_o - h_i)}{4 \ L_h} \quad \text{so that} \quad \frac{T_o - T_i}{T_{sat} - T_i} = \frac{1}{1 + \left(32.5 \, D_h / L_h\right)} \tag{2}$$

$$q_{OFI-SZ} = -G\,h_{fg,o}\,X_o\,Max\left(\frac{455}{Pe}, 0.0065\right) \qquad \text{where} \quad Pe = \frac{G\,D_h\,C_{pf,o}}{K_{f,o}} \tag{3}$$

$$q_c(D_h, P, G, X_o) = \begin{cases} q_c(0.008, P, G, X_o)\left(\dfrac{0.008}{D_h}\right)^{0.312} & \text{if } G \leq 8000 \\[3mm] q_c(0.008, P, 8000, X_o)\left(\dfrac{0.008}{D_h}\right)^{0.312}\left(\dfrac{G}{8000}\right)^{0.376} & \text{if } G > 8000 \end{cases} \tag{4}$$

$$\frac{q_c}{G\,h_{fg,o}} = \frac{C_1\left(\dfrac{G^2 D_e}{\rho_f\,\sigma}\right)^{C_2}(\rho_f/\rho_g)^{C_3}\left[1 - C_4\left(\rho_f/\rho_g\right)^{C_5} X_i^*\right]}{1 + 4C_1 C_4\left(\dfrac{G^2 D_e}{\rho_f\,\sigma}\right)^{C_2}(\rho_f/\rho_g)^{C_3+C_5}(L_h/D_h)} \tag{5}$$

where $C_1 = 0.0722$, $C_2 = -0.312$, $C_3 = -0.644$, $C_4 = 0.900$, $C_5 = 0.724$, $X_i^* = (h_i - h_{fo})/h_{fg,o}$, and D_h and D_e are heated and hydraulic diameters.

The five safety margins were calculated iteratively, using the heat balance method (HBM) as agreed upon in 1996 by a panel of experts (Celata, Groeneveld, Hejzlar and Todreas, and Inasaka and Nariai) [10, 11], for given values of the five independent parameters: exit pressure, heated length, heated diameter, inlet temperature, mass flux. The coolant properties were calculated using the property subroutines of the PLTEMP/ANL code [12, 13]. Additional details are given in [1]. The safety margins were calculated for mass flux over the range 1000 to 30,000 kg/m²-s (i.e., the coolant velocity range of approximately 1 to 30 m/s) for the following values of independent parameters (3 heated lengths × 6 exit pressures × 4 heated diameters × 3 inlet temperatures, i.e., altogether 216 cases):

3 heated lengths $L_h = 0.28, 0.61, 1.18$ m   6 exit pressures P = 1, 5, 10, 20, 30, 50 bar
4 heated diameters $D_h = 3, 4, 6, 8$ mm   3 inlet temperatures $T_{in} = 30, 50, 70$ ° C

CHFs Calculated by the extended Groeneveld Table and the Hall-Mudawar ICC: To verify the accuracy of the extended Groeneveld 2006 CHF Table, it was compared with the Hall-Mudawar ICC for all the above 216 cases. Figure 1a shows a typical comparison between the two CHF prediction methods, for all the 72 cases of heated length 0.61 m. The actual number of data points plotted in Fig. 1a is less than the total number 2160 (= 72 × 30) because the Hall-Mudawar ICC holds only for exit quality $X_o \leq 0$ (subcooled CHF). The comparison of the two CHF prediction methods for each of the 216 cases as a function of mass flux was also plotted [1], and one of 36 such plots is shown in Fig. 2a. The RMS difference between the two methods is 8.5 %, 8.6 %, and 8.8 % for the heated lengths of 0.28, 0.61, and 1.18 m respectively (Table 1). In conclusion, there is a close agreement between the two prediction methods. The extended Groeneveld Table is selected because it is also applicable to saturated CHF ($X_o \geq 0$).

OFIs Calculated by the Whittle-Forgan and the Saha-Zuber Correlations: To verify the accuracy of the Whittle-Forgan OFI correlation, it was compared with the Saha-Zuber correlation for all the 216 cases. Figure 1b shows a typical comparison between OFI heat fluxes by the Whittle-Forgan ($\eta = 32.5$) and the Saha-Zuber correlations, for all the 72 cases of heated length 0.61 m.

The plot consists of 2160 data points (72 cases $\times$ 30 mass fluxes from 1000 to 30000 kg/m^2-s). The comparison of the two OFI prediction methods for each of 216 cases as a function of mass flux, was also plotted [1], and one of 36 such plots is shown in Fig. 2b. The difference over the 72 cases of each heated length is given in Table 1. The RMS difference between the two methods is 5.2 %, 3.0 %, and 1.8 % for the heated lengths of 0.28, 0.61, and 1.18 m respectively. In conclusion, there is a close agreement between the two OFI prediction methods. The Whittle-Forgan (with η = 32.5) is selected because statistical analyses at ANL [13] and IAEA have recommended it.

3. Margin between CHF and OFI

The critical heat flux (CHF) is the maximum heat flux that can be transferred from the heated wall to the coolant, with all independent parameters (P, G, L_h , D_h , T_{in}) kept constant. In order to measure the true CHF, the test loop must be stiff so that the coolant mass flux (G) does not decrease due to the increase in flow resistance caused by boiling.

The onset of static flow instability (OFI) is defined as the minimum ΔP point on the plot of ΔP versus flow rate of subcooled boiling liquid in a heated channel. OFI is caused by lack of a hydraulic equilibrium point (on the ΔP versus flow plot) between the ΔP demanded by the heated channel and the ΔP supplied by the pump. The onset of significant void (OSV), i.e., onset of bubble departure from the heated wall, generally occurs prior to OFI at a slightly higher flow than the OFI on the ΔP versus flow plot [5]. This was also tentatively concluded earlier by Whittle-Forgan [4]. As a result, an OSV correlation is used to provide a conservative estimate of OFI [5]. The Saha-Zuber correlation [6] has been quite successful in predicting various experimental data for OSV and OFI [5].

4. Some Cases Where CHF Occurs Before OFI

Four CHF mechanisms during boiling in conditions ranging from high subcooling to high quality and in different flow patterns are summarized in [1]. One of these mechanisms is the occurrence of CHF before bubble detachment (i.e., OFI), as observed in high-speed (20000 frames/s) photographic study of bubbles in *highly subcooled* nucleate boiling of water and its approach to CHF by Gunther [14, 15] and Celata et al. [16]. These experiments and the analysis of some of them by Bankoff [17] are also summarized in [1].

While developing a CHF correlation using *true* quality (instead of the thermodynamic quality used in most CHF correlations), Shim et al. [18] stated that there was a small number of CHF data (72 out of 8912 CHF data in their database), for highly subcooled flow with high mass flux, in which CHF occurs *before* OSV. They noted that their CHF model failed for these CHF data and hence they had to exclude the data from the analysis. Since OFI occurs soon *after* OSV, the existence of these CHF data shows that CHF can occur before OFI for highly subcooled flow with high mass flux.

Table 1. Difference between CHFs Calculated by the Extended Groeneveld Table and the Hall-Mudawar ICC, and Difference between OFIs Calculated by Whittle-Forgan and Saha-Zuber Correlations

|	% Difference	
	Gro CHF vs. H-M CHF	W-F OFI vs. S-Z OFI [a]
	For 0.28 m Heated Length	
Number of Data Points	1881	2088
Mean Difference %	-2.84	-4.67
Max Absolute Diff. %	40.6	11.1
Case / Mass Flux [b]	67/6000	2/2000
RMS Difference %	8.50	5.19
	For 0.61 m Heated Length	
Number of Data Points	1448	2088
Mean Difference %	-5.75	-2.68
Max Absolute Diff. %	38.7	5.66
Case / Mass Flux [a]	67/18000	2/2000
RMS Difference %	8.56	3.03
	For 1.18 m Heated Length	
Number of Data Points	845	2088
Mean Difference %	-7.40	-1.54
Max Absolute Diff. %	28.0	3.16
Case / Mass Flux [a]	43/23000	67/5000
RMS Difference %	8.81	1.77

a. For $G > 1000$ kg/m^2-s

b. Case number (see Table 4 of [1]) and mass flux of the data point that has the maximum absolute difference
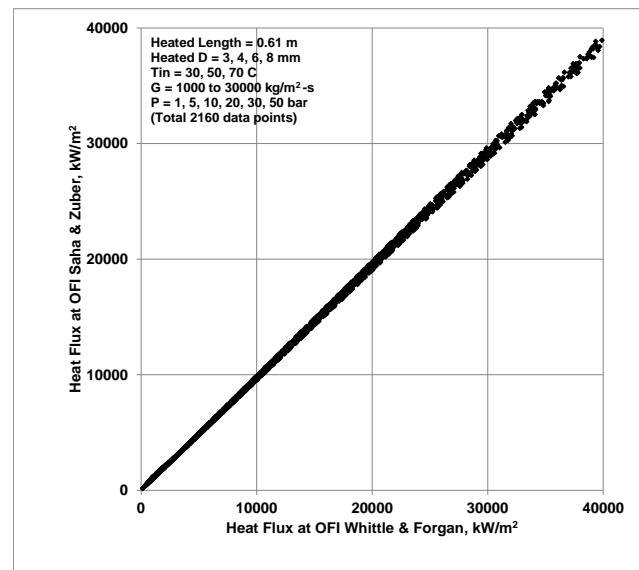
Gro   = Extended Groeneveld 2006 Table,

H-M   = Hall-Mudawar Inlet Conditions Correlation

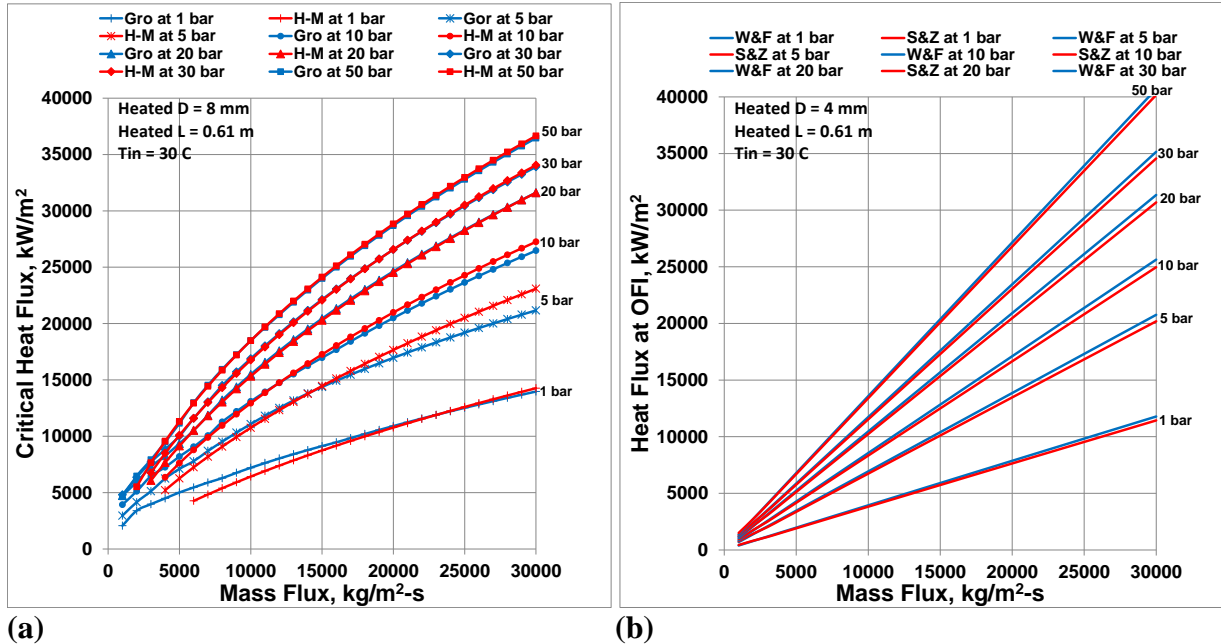W-F   = Whittle-Forgan ($\eta = 32.5$),

S-Z   = Saha-Zuber
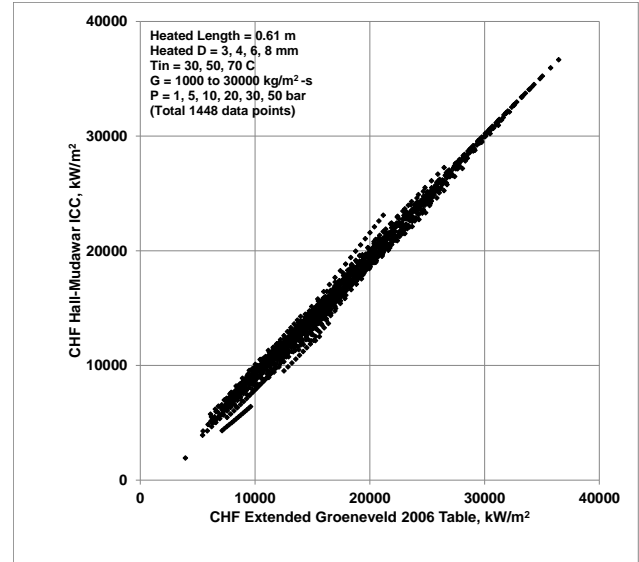
(a)

(b)

Fig. 1.   (a) Comparison between CHFs by the Extended Groeneveld 2006 Table and the Hall-Mudawar ICC for 72 Cases of $L_h = 0.61$ m, and (b) Comparison between OFI Heat Fluxes by Whittle-Forgan ($\eta = 32.5$) and Saha-Zuber Correlations for 72 Cases of $L_h = 0.61$ m

(a)   **(b)**

Fig. 2. Comparison of (a) the Extended Groeneveld 2006 CHF Table and the Hall-Mudawar Inlet Conditions Correlation at D_h = 8 mm; (b) OFI Heat Fluxes by Whittle-Forgan (η=32.5) and Saha-Zuber Correlations at D_h = 4 mm

The order of occurrence of CHF and OFI was studied earlier [7] by calculating the thermodynamic quality at OSV (X_{osv}) for the tabulated values of subcooled CHF in the Groeneveld 2006 Table for a tube of 8 mm diameter at 5 bar pressure. X_{osv} was calculated using the Saha-Zuber correlation on Excel spreadsheet for the CHF values in the Groeneveld Table. The calculated X_{osv} was compared with the exit quality X_o given in the Groeneveld Table corresponding to the CHF. If X_{osv} is less than X_o, then OFI occurs before CHF, and if X_{osv} is greater than X_o, then the reverse occurs (CHF occurs before OFI). It is found that highly subcooled flow with high mass flux leads to CHF occurring before OFI. An example of this calculation follows:

The CHF is 13200 kW/m^2 at X_o = -0.15, G = 8000 kg/m^2-s in the Groeneveld 2006 Table at 5 bar for a tube of 8 mm diameter. The heated length calculated by heat balance assuming an inlet temperature of 30 °C is found to be 0.24 m. For this channel, the onset of significant voids by the Saha-Zuber correlation is found to occur at heat flux 14997 kW/m^2 and quality X_{osv} = -0.137. Comparing the qualities, OFI occurs at a higher quality (–0.137) compared to the quality (–0.15) at which CHF occurs, implying that CHF occurs prior to OFI.

5. Comparison of Heat Fluxes at ONB, OFI, and CHF

The relative magnitudes of the selected three safety margins (i.e., the Bergles and Rohsenow ONB heat flux, the Whittle-Forgan OFI heat flux, and the CHF by the extended Groeneveld 2006 Table) are shown together in 18 plots in [1]. It is found that the OFI heat flux intersects with the CHF at a certain mass flux and heat flux. The intersection occurs at lower and lower mass fluxes (G) as the exit pressure increases from 1 to 50 bar. The point of intersection is called

the reversal point [19]. The corresponding mass flux and heat flux are referred to as the reversal mass flux (G_{rev}) and reversal heat flux (q_{rev}).

To reduce clutter, only the Whittle-Forgan OFI heat flux and the extended Groeneveld Table CHF are plotted in Fig. 3 to display the effect of exit pressure on the intersection of the OFI heat flux and CHF. The locus of the point of intersection is also shown in Fig. 3. The mass flux G_{rev} and heat flux q_{rev} at the intersection point depend on the channel exit pressure. Six such plots for different combinations of D_h and L_h typical of research reactors (D_h = 4, 8 mm; L_h = 0.28, 0.61, 1.18 m) are given in [1].
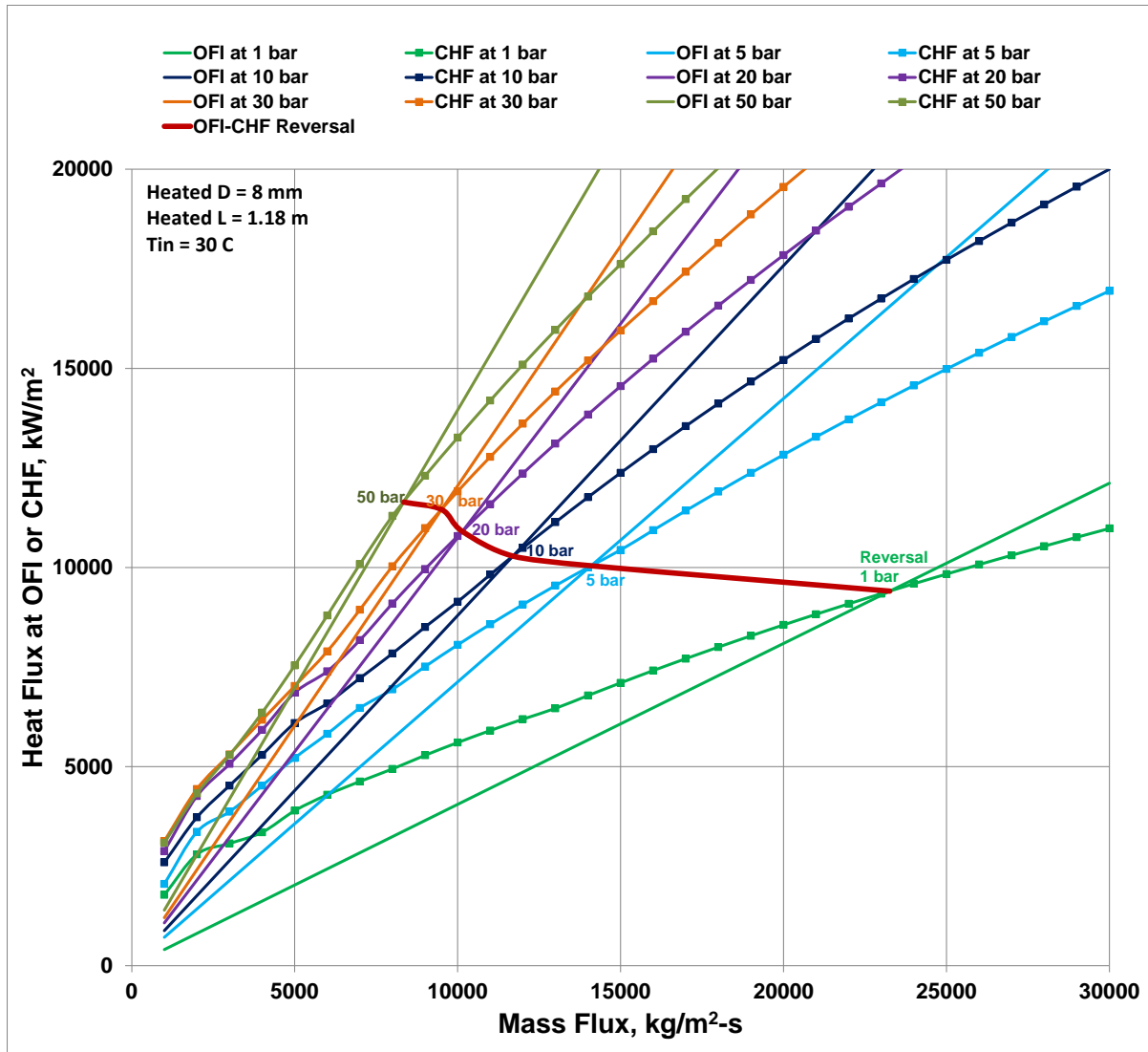
Fig. 3. Intersection of OFI Heat Flux and CHF at Exit Pressures of 1 to 50 bar

The intersection is referred to as the reversal because the OFI heat flux is smaller than the CHF for mass fluxes $G < G_{rev}$ whereas for mass fluxes $G > G_{rev}$ the CHF is smaller than the OFI heat flux. It means that the channel power is OFI-limited for $G < G_{rev}$ and CHF-limited for $G > G_{rev}$, i.e., a reversal in the roles of OFI and CHF occurs at the intersection. To make an OFI-CHF

reversal diagram that is useful for scoping whether a reactor is OFI-limited or CHF-limited, several combinations of T_{in}, D_h and L_h as well as several values of exit pressure need to be plotted in a single figure. A method of doing this is by reversal diagrams, as given below.

6. OFI-CHF Reversal Diagrams

Instead of plotting OFI heat flux and CHF (as in Fig. 3), only the mass flux at their intersection is plotted as a function of the exit pressure in Fig. 4, for all 12 combinations of T_{in} and D_h ($T_{in} = 30$, 50, 70 °C, $D_h = 3, 4, 6, 8$ mm), for a given fixed L_h in a figure ($L_h = 0.28, 0.61, 1.18$ m). This was done to put more calculated results in a single figure. Figure 4a shows the reversal mass flux (G_{rev}) for $L_h = 0.61$ m, and Fig. 4b the corresponding reversal heat flux (q_{rev}). Similar diagrams for $L_h = 0.28$ m and 1.18 m are also available, with all the data plotted in these diagrams [1].

Figure 4 was developed assuming axially uniform heat flux. The justification for its application to reactors with axially non-uniform heat flux is discussed in Section 7. It can be used only to scope whether a research reactor is OFI-limited or CHF-limited based on five characteristics of its coolant channel: the heated length, heated diameter, inlet temperature, exit pressure, and mass flux. Figure 4 cannot replace the detailed thermal-hydraulic analysis that is required to design a research reactor.

The meaning of Fig. 4 can be explained by considering an example research reactor having a heated length of 0.61 m (24 inches) and a channel heated diameter of 4 mm, operating at a coolant exit pressure of 40 bar, inlet temperature of 30 °C, and mass flux of 10000 kg/m²-s. The point R (at the operating mass flux of 10000 kg/m²-s) on the vertical line AB drawn at 40 bar represents this research reactor on Fig. 4a. The point B is the intersection of this vertical line with the OFI-CHF reversal mass flux curve applicable to this reactor, i.e., the curve corresponding to the reactor's heated diameter and inlet temperature (4 mm and 30 °C). The point B gives the mass flux at the OFI-CHF reversal.

To find whether the research reactor in question is OFI-limited or CHF-limited, one checks in Fig. 4a whether the point R is below or above the point B. If the point R representing the reactor lies below (i.e., the operating mass flux is less than the reversal mass flux), the reactor in question is OFI-limited. If the point R is above, the reactor is CHF-limited.

If the point R in Fig. 4a is below the applicable reversal curve (OFI-limited reactor), then an estimate of the maximum allowed heat flux (averaged over the heated length) is given by Fig. 4b as follows. The reversal mass flux, G_{rev}, at point B of Fig. 4a (upper graph) corresponds to the reversal heat flux, q_{rev}, provided by point C of Fig. 4b (lower graph). Since the heat flux at OFI is approximately proportional to the mass flux at OFI, the OFI heat flux, q_{OFI}, at the operating mass flux, G, is estimated to be $q_{rev}(G/G_{rev})$. The maximum allowed heat flux for this OFI-limited reactor equals q_{OFI}, i.e., be $q_{rev}(G/G_{rev})$. This heat flux times L_hP_h gives the OFI power, or the maximum allowed power of the channel, without accounting for uncertainties. In the other case, if the point R in Fig. 4a lies above the reversal mass flux curve applicable to the reactor, the maximum allowed reactor power is more than the power determined by the reversal heat flux (q_{rev}), and its value will be determined by the CHF at the operating mass flux G.
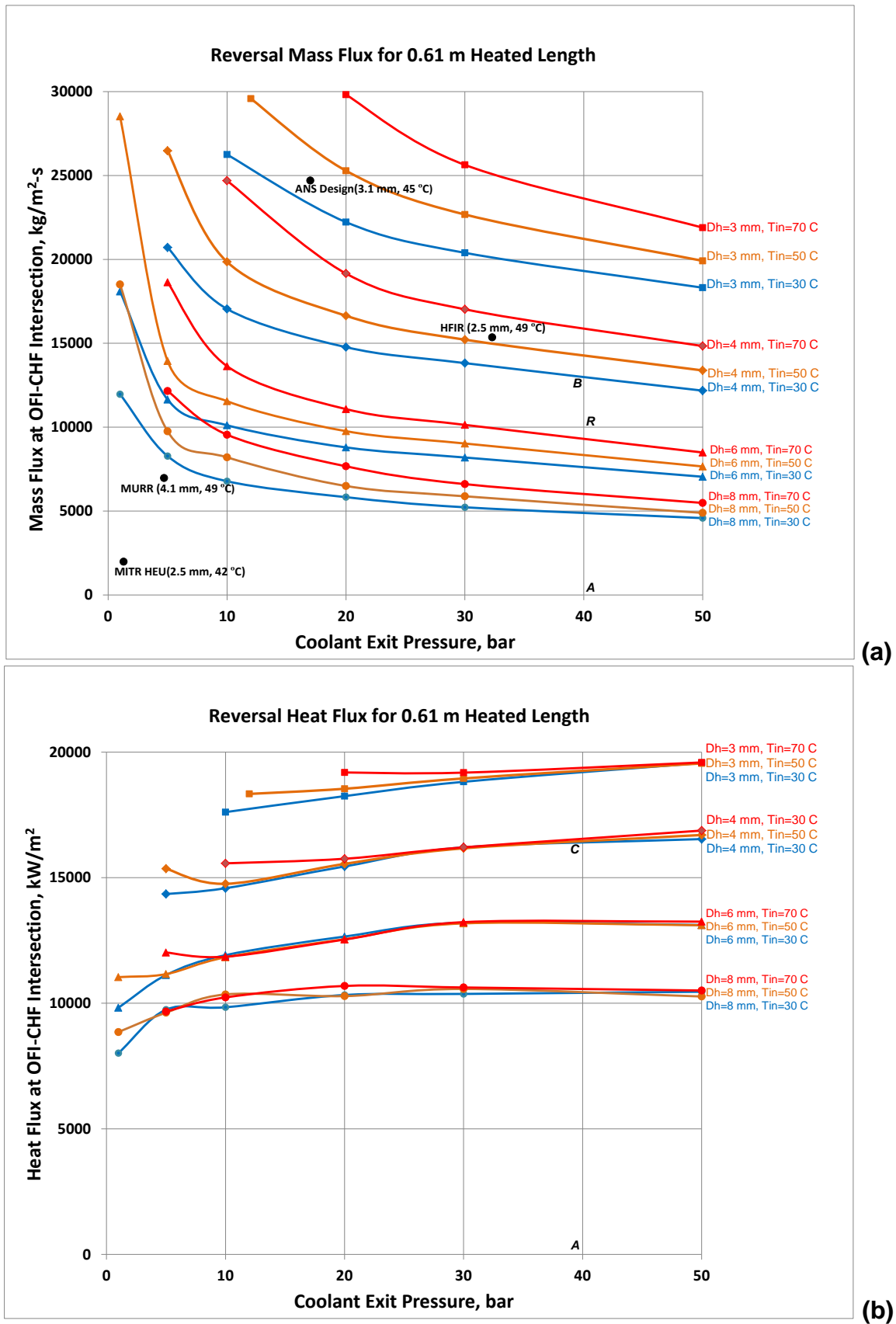
Fig. 4. Reversal Diagram for 0.61 m Heated Length: (a) Mass Flux and (b) Heat Flux at OFI-CHF Intersection. The parentheses near the point representing a reactor contain the heated diameter and inlet temperature which determine the reversal line applicable to the reactor.

7. Applicability of the Reversal Diagram to Axially Non-uniform Heat Flux

The heat flux was assumed to be axially uniform in the development of the reversal diagrams. However, due to the two reasons noted below, a channel having an axially non-uniform heat flux distribution may be replaced by an equivalent channel having an axially uniform heat flux equal to the average heat flux, and the reversal diagrams are applicable to the equivalent channel.

(1) According to the widely used Whittle-Forgan flow instability criterion, the power removed by the coolant from a channel at OFI depends only on the coolant inlet-to-outlet temperature rise, and not on the axial shape of heat flux. This means that the actual heat flux distribution of the channel can be replaced, for OFI power calculation purposes, by a uniform heat flux equal to the axially averaged value of the actual heat flux distribution.

(2) Similarly, the overall CHF power hypothesis of Lee and Obertelli [20, 21] suggests that the total power which can be fed to a tube with axially non-uniform heat flux distribution before CHF, is the same as the CHF power for a uniformly heated tube of the same inner diameter, heated length, and inlet conditions. Of the two methods of handling axially non-uniform heat flux distribution, the local conditions hypothesis and the overall power hypothesis, it is found that the latter is slightly more accurate for symmetrical heat flux profiles. This means that the actual heat flux distribution of a channel can be replaced, for CHF power calculation purposes, by a uniform heat flux equal to the axially averaged value of the actual heat flux distribution.

8. Application of OFI-CHF Reversal Diagram to Research Reactors

The OFI-CHF reversal diagram is applied to 5 research reactors, to scope whether they are OFI-limited or CHF-limited. The five key reactor parameters (L_h, P, G, D_h, T_{in}) required for this purpose are listed in Table 2. The values of P and G are plotted on Fig. 4a to get a point representing each reactor. Four reactors (the ANS Design, the HIFR, the MITR, and the MURR) are plotted on the reversal diagram in Fig. 4a for a heated length of 0.61 m. The Advanced Test Reactor (ATR) was plotted on the reversal diagram for a heated length of 1.28 m in [1].

Two limitations of this scoping should be noted:

(1) The development of reversal diagrams used best-estimate values of CHF and OFI heat flux. It does not allow for regulatory requirements like CHF ratio ≥ 2.0. Such a requirement practically reduces the best-estimate of CHF in reactor analysis, and its effect is significant.
(2) The effect of uncertainties in coolant mass flux and channel exit pressure, if available, may be accounted for by plotting a rectangle (rather than a point) to represent a coolant channel. However, these uncertainties require a complete thermal-hydraulic analysis, and therefore are not available for scoping without any calculation.

The heated diameter and inlet temperature of these reactors do not match those of one of the reversal lines plotted on the OFI-CHF diagram. Hence one needs to interpolate between a suitable pair of reversal lines. During the interpolation, the trends to keep in mind are: The reversal line shifts down if the heated diameter increases, or if the inlet temperature decreases, or if the heated length decreases. The points representing these 5 reactors are below the OFI-CHF

reversal mass flux curve applicable to the reactor, indicating that these reactors are OFI-limited. These scoping results are in agreement with the results of detailed thermal-hydraulic analyses by the different responsible organizations, as reported in the references shown in Table 2.

Table 2. Key Parameters of Some Experimental Reactors Plotted on the OFI-CHF Reversal Diagram of Fig. 4

D_h = Heated diameter, D_e = Hydraulic diameter,   C = Under construction,
D = Reactor design,   O = Operational reactor,   S = Shutdown reactor

No.	Reactor	Status	Power	Exit Pres.	Coolant Vel.	Mass Flux	D_e	D_h	Heated Length	T_{in}	OFI/CHF Limited?
			MW_{th}	bar	m/s	kg/m^2-s	mm	mm	m	°C	
1	ANS Design, USA[23]	D	350	17	25.0	24700	2.54	3.05[a]	0.474	45	OFI
2	HFIR, USA[24]	O	85	32.3	15.4	15355		2.54	0.508	49	OFI
3	MITR, HEU Core, USA[25]	O	6	1.30	2.0	1980	2.19	2.48	0.568	42	OFI
4	MURR, USA[26]	O	10	4.70	7.00	6969		4.06	0.610	49	OFI
5	ATR, USA[27]	O	250	18.8	14.60	14552		3.94	1.181	51.7	OFI

a. The heated diameter was estimated as 1.2 times the hydraulic diameter.

9. Conclusions

Photographic experimental evidence is provided for CHF occurring before bubble detachment from the heated wall (i.e., before OFI) in highly subcooled (ΔT_{sub} > ~85 °C) flow boiling. The OFI heat flux and CHF are calculated using the state-of-the-art prediction methods in the coolant mass flux range of 1000 to 30000 kg.m^2-s, for 216 cases covering the typical parametric range of research reactors: channel exit pressure 1 to 50 bar, heated diameter 3 to 8 mm, heated length 0.28 to 1.18 m, inlet temperature 30 to 70 °C. Based on the comparison of the OFI heat flux and CHF, the safety limits imposed by OFI and CHF are found to cross over in a consistent manner.

For each heated length of interest, a diagram showing the mass flux at the intersection of OFI heat flux and CHF (the reversal mass flux) is plotted as a function of exit pressure, with heated diameter and inlet temperature as parameters. The reversal diagram was developed for coolant channels with axially uniform heat flux. The basis for the applicability of the diagram to reactors with axially non-uniform axial power shapes is provided. The diagram is used to scope whether a research reactor coolant channel is OFI-limited or CHF-limited based on five key parameters: the heated length, heated diameter, inlet temperature, exit pressure, and mass flux. To scope a reactor, it is represented by a point on the reversal diagram, based on the exit pressure and mass flux of its hot channel. If the plotted point is below the applicable reversal line corresponding to the channel heated diameter and inlet temperature, the channel is OFI-limited. If the plotted point is above the applicable reversal line, the channel is CHF-limited.

The points representing five reactors (see Table 2) are below the OFI-CHF reversal mass flux curve applicable to the reactor, indicating that all these reactors are OFI-limited. These scoping results are in agreement with the results of detailed thermal-hydraulic analyses reported by the different organizations operating these reactors.

There is a close agreement between CHFs predicted by the extended Groeneveld 2006 Table and the Hall-Mudawar ICC. There is a close agreement between the Whittle-Forgan (using $\eta = 32.5$) and the Saha-Zuber OFI prediction methods.

ACKNOWLEDGEMENTS

10. References

1. M. Kalimullah, A. P. Olson, E. E. Feldman, and J. E. Matos, "Reversal of OFI and CHF in Research Reactors Operating at 1 to 50 bar," ANL/GTRI/TM-13/14, Nuclear Engineering Division, Argonne National Laboratory, Argonne, IL, USA (September 15, 2013).
2. A.E. Bergles and W.M. Rohsenow, "The Determination of Forced-Convection Surface-Boiling Heat Transfer," J. Heat of Transfer, Vol. 86, pp. 365–372 (1964).
3. N. Basu, G. R. Warrier, and V. K. Dhir, "Onset of Nucleate Boling and Active Nucleation Site Density During Subcooled Flow Boling," J. Heat of Transfer, Vol. 124, pp. 717-728 (2002).
4. R. H. Whittle and R. Forgan, "A Correlation for the Minima in the Pressure Drop vs. Flow Rate Curves for Subcooled Water Flow in Narrow Heated Channels," Nuclear Eng. and Design, Vol. 6, pp. 89-99 (1967).
5. J. E. Kennedy, G. M. Roach, Jr., M. F. Dowling, S. I. Abdel-Khalik, S. M. Ghiaasiaan, S. M. Jeter, and Z. H. Qureshi, "The Onset of Flow Instability in Uniformly Heated Horizontal Microchannels," Transactions of the ASME, Vol. 122, pp. 118-125 (2000).
6. P. Saha and N. Zuber, "Point of Net Vapor Generation and Vapor Void Fraction in Subcooled Boiling," Proc. of 5th Intern. Heat Transfer Conf., Vol. 4, Tokyo, pp. 175-179 (1974).
7. M. Kalimullah, E. E. Feldman, A. P. Olson, B. Dionne, J. G. Stevens, and J. E. Matos, "An Evaluation of Subcooled CHF Correlations and Databases for Research Reactors Operating at 1 to 50 bar Pressure," RERTR 2012, 34th Intern. Meeting on Reduced Enrichment for Research and Test Reactors, Warsaw, Poland (October 14-17, 2012).
8. D. C. Groeneveld, J. Q. Shan, A. Z. Vasic, L. K. H. Leung, A. Durmayaz, J. Yang, S. C. Cheng, and A. Tanase, "The 2006 CHF Look-up Table," Nucl. Eng. and Design, Vol. 237, pp. 1909-1922 (2007).
9. D. D. Hall and I. Mudawar, "Critical Heat Flux for Water Flow in Tubes – II. Subcooled CHF Correlations," Intern. J. Heat and Mass Transfer, Vol. 43, pp. 2605-2640 (2000).
10. G. P. Celata, "On the Application Method of Critical Heat Flux Correlations," Letter to the Editor, Nuclear Eng. Design, Vol. 163, pp. 241-242 (1996).
11. P. Hejzlar and N. E. Todreas, "Consideration of Critical Heat Flux Margin Prediction by Subcooled or Low Quality Critical Heat Flux Correlations," Nucl. Eng. Design, Vol. 163, pp. 215-223 (1996).
12. "International Association for the Properties of Steam (IAPS)," H. J. White, Secretary, National Bureau of Standards, Washington, D.C., 1977 (revised 1983).
13. A. P. Olson and M. Kalimullah, "A User's Guide to the PLTEMP/ANL Code," ANL/RERTR/TM-11-22, Version 4.11, Nuclear Engineering Division, Argonne National Laboratory, Argonne, IL, USA (November 15, 2011).

14. F. C. Gunther, "Photographic Study of Surface-Boiling Heat Transfer to Water with Forced Convection," Progress Report No. 4-75, Jet Propulsion Laboratory, California Institute of Technology, Pasadena, California, USA (1950).

15. F. C. Gunther, "Photographic Study of Surface-Boiling Heat Transfer to Water with Forced Convection," Transactions of ASME, Vol. 73, pp. 11 5-123 (February 1951).

16. G. P. Celata, M. Cumo, A. Mariani, and G. Zummo, "Burnout in Subcooled Flow Boiling of Water, A Visual Experimental Study," Intern. Journal of Thermal Sciences, Vol. 39, pp. 896-908 (2000).

17. S. G. Bankoff, "On the Mechanism of Subcooled Nucleate Boiling, Parts I and II," Chem. Eng. Progress Symposium Series, Vol. 57, No. 32, pp. 156-172 (1961).

18. W. J. Shim and J. Park, "Analysis of a Generalized CHF Model in Vertical Round Tubes with Uniform Heat Flux," J. Ind. Eng. Chem., Vol. 9, pp. 607-613 (2003).

19. M. Siman-Tov, D. K. Felde, J. L. McDuffee, and G. L. Yoder, "Experimental Study of Static Flow Instability in Subcooled Flow Boiling in Parallel Channels," 4th. ASME/JSME Thermal Engineers Joint Conference, Maui, Hawaii (January 1995).

20. J. G. Collier and J. R. Thome, "Convective Boiling and Condensation," 3rd Edition, Clarendon Press, Oxford, Section 9.2.1.2 (1994).

21. D. H. Lee and J. D. Obertelli, "An Experimental Investigation of Forced Convection Burnout in High Pressure Water – Part II," Report UK AERE-R-309, Atomic Energy Research Establishment, Harwell, England (1963).

22. Constantine P. Tzanos, Heat Transfer Predictions by Turbulence Models and Heat Transfer Correlations, Trans. ANS 105, American Nuclear Society (November 2011).

23. G. L. Yoder, Jr., et al., "Steady-State Thermal-Hydraulic Analysis of the Advanced Neutron Source Reactor," ORNL/TM-12398, Oak Ridge National Laboratory, Tennessee May 1994).

24. H. A. McLain, "HFIR Fuel Element Steady-State Heat Transfer Analysis, Revised Version," ORNL-TM-1904, Oak Ridge National Laboratory, Oak Ridge, Tennessee, USA (December 1967).

25. K. Y. Chiang, "Thermal Hydraulic Limits Analysis for the MIT Research Reactor Low Enrichment Uranium Core Conversion Using Statistical Propagation of Parametric Uncertainties," Thesis for Master of Science Degree, Certified and Accepted by L. W. Hu, B. Forget, T, Newton, and M. S. Kazimi, Department of Nuclear Science and Engineering, Massachusetts Institute of Technology, Cambridge, MA, USA (June 2012).

26. Feldman, E. E., et al., Technical Basis in Support of the Conversion of the University of Missouri Research Reactor (MURR) Core from Highly-Enriched to Low-Enriched Uranium – Steady-State Thermal-Hydraulic Analysis, ANL/RERTR/TM-12-37, Revision 1, Argonne National Laboratory, Argonne, IL (January 2013).

27. S. A. Atkinson, "A Forced Convection DNB Correlation for Stainless Steel or Aluminum Heaters for Low Subcooling Based on Savannah River Laboratory Data," TR-813, Aerojet Nuclear Company, Idaho Falls, ID (March 25, 1976).